Angular Distributions of the D(d,n)He^3 Reaction for 5- to 12-Mev Deuterons

MURREY D. GOLDBERG AND JAMES M. LE BLANC
Lawrence Radiation Laboratory, University of California, Livermore, California
(Received April 21, 1960)

The absolute differential cross section for production of monoenergetic neutrons by the D(d,n)He^3 reaction has been measured with 5.0-, 7.6-, 9.6-, and 12.2-Mev deuterons. A proton recoil counter telescope was used to detect the neutrons and to separate neutrons from the D(d,np)D breakup reaction. The angular distributions at all energies are very peaked in the forward direction, with a first minimum around 30 to 40 degrees and a subsequent smaller maximum. The angular distributions, transformed to the center-of-mass system, have been fitted with the exchange stripping theory of Owen and Madansky, in which stripping from both incident and target deuterons is formally included. Excellent fits were obtained, but it was necessary to monotonically decrease the interaction radius, R_0, with incident deuteron energy. The variation was considerable, from $R_0=8.4\pm0.2$ fermi at 5.0 Mev to $R_0=5.5\pm0.2$ fermi at 12.2 Mev. An isotropic contribution of about 3 mb/sr was added to each distribution to obtain the best fit.

INTRODUCTION

THE D(d,n)He^3 reaction provides a copious source of monoenergetic fast neutrons, and thus is an important experimental tool. A knowledge of the angular yield of neutrons from this reaction is therefore of considerable use. From the theoretical point of view, the reaction lends itself to a stripping analysis and might also provide additional information on the four-nucleon system.

Much experimental work has been done on this reaction and its companion, the D$(d,p)T$ reaction.[1] At deuteron energies greater than 5 Mev, two recent D(d,n)He^3 experiments have been reported. Brolley, Putnam, and Rosen,[2] using a nuclear emulsion camera, measured angular distributions at incident deuteron energies of 6, 8, 10, 12, and 14 Mev. Since they were detecting the He^3 residual nuclei, they were unable to investigate the forward peak at center-of-mass angles less than about 20°. Daehnick and Fowler,[3] using a single plastic scintillator as a neutron detector, obtained an angular distribution at a deuteron energy of 8.4 ± 0.1 Mev for center-of-mass angles from 2° to 84°.

The theoretical work of Konopinski *et al.*[4,5] showed that the measured angular distributions could be understood in terms of spin-orbit forces and centrifugal barriers for the deuteron partial waves, and that the measured distributions could be decomposed into a sum of Legendre polynomials (even orders only), the coefficients of which indicate the contribution of each partial wave.

Fairbairn[6] has considered the d-D reaction from the point of view of Butler[7] stripping, properly accounting for the identity of the incident and target particles. His predicted angular distribution showed qualitative agreement with experiment at forward angles for 19-Mev deuterons, but his predicted variation of the 0° cross section with energy was opposite to the experimentally observed variation.

The exchange stripping model of Owen and Madansky[8,9,3] can be applied to the angular distribution of D(d,n)He^3 neutrons. In this model, the contribution to the angular distribution of stripping from the "heavy particle" (in this case, the target deuteron) is formally included. A fitting of the angular distributions reported here has been made using this approach.

APPARATUS

Two separate experiments were performed. First, the angular yield of D(d,n)He^3 neutrons was measured,

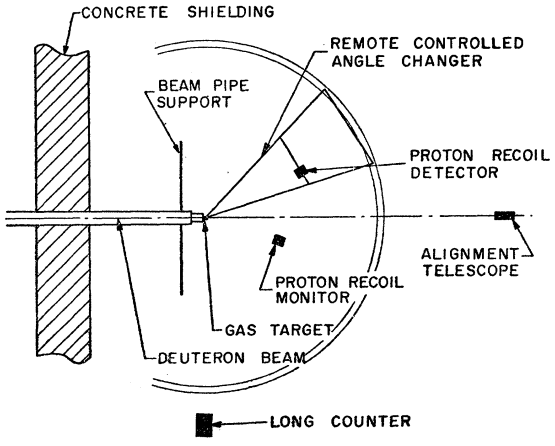

FIG. 1. Schematic plan view of layout of experimental equipment for angular yield measurements.

* This work was done under the auspices of the U. S. Atomic Energy Commission.

[1] A review of work on the neutron producing reaction as well as a thorough bibliography, is given in a paper by J. L. Fowler and J. E. Brolley, Jr., Revs. Modern Phys. **28**, 103 (1956).

[2] J. E. Brolley, Jr., T. M. Putnam, and L. Rosen, Phys. Rev. **107**, 820 (1957).

[3] W. W. Daehnick and J. M. Fowler, Phys. Rev. **111**, 1309 (1958).

[4] E. J. Konopinski and E. Teller, Phys. Rev. **73**, 822 (1948).

[5] F. M. Beiduk, J. R. Pruett, and E. J. Konopinski, Phys. Rev. **77**, 622 (1950).

[6] W. M. Fairbairn, Proc. Phys. Soc. (London) **A67**, 990 (1954).

[7] S. T. Butler, Proc. Roy. Soc. (London) **A208**, 559 (1951).

[8] George E. Owen and L. Madansky, Phys. Rev. **105**, 1766 (1957).

[9] George E. Owen and L. Madansky, Am. J. Phys. **26**, 260 (1958).

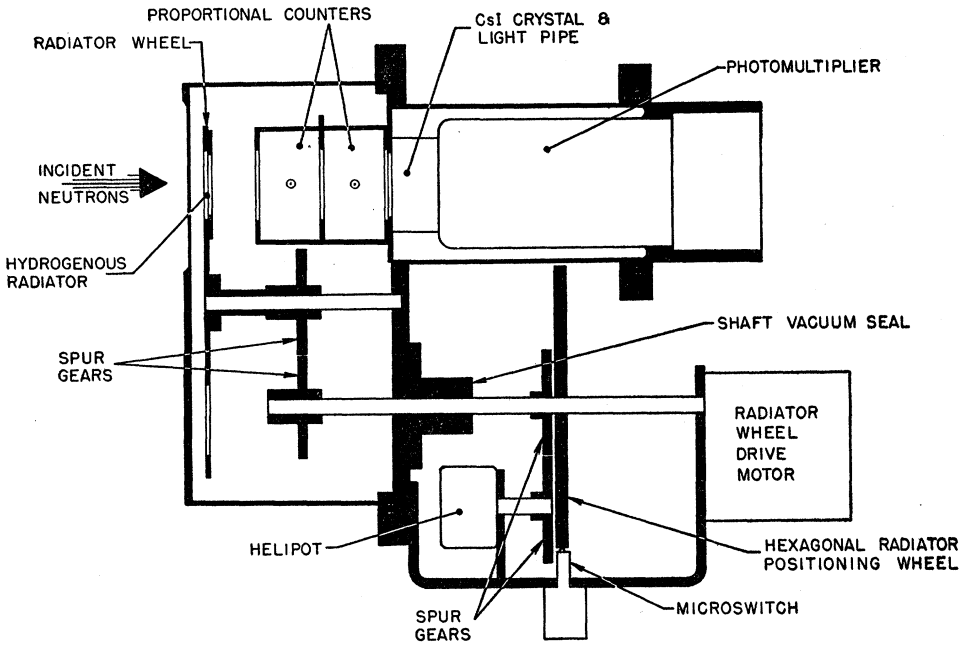

FIG. 2. Schematic of proton recoil counter telescope. Six positions are available on the radiator wheel, and the radiator wheel drive motor is remotely controlled. Closure of the microswitch by the hexagonal positioning wheel indicates when a radiator is in position, and the current through the helipot indicates which radiator is in position. The radiator-CsI crystal spacing can be varied by moving the crystal phototube back.

relative to the yield at 0°, at four incident deuteron laboratory energies, 5.0, 7.6, 9.6, and 12.2 Mev. Second, absolute cross sections at 0° were measured at several incident energies between 3.4 and 10.2 Mev. The relative angular yield curves were subsequently normalized to the best 0° cross sections measured in the second experiment.

A plan view of the experimental layout for the relative angular yield experiment is shown schematically in Fig. 1. The deuteron beam is that of the Livermore 90-inch variable-energy cyclotron.

The gas target has two atmospheres of D_2 gas within a stainless steel cylindrical container 4 inches in length and 1 inch in diameter. A 0.020-inch tantalum beam stopper at the end of the container prevents deuteron bombardment of the stainless steel end wall. The deuterons enter the target through a 0.00025-inch (about 10 mg/cm²) tantalum foil. Tantalum collimators, $\frac{1}{2}$ inch in diameter, properly placed in the beam pipe, prevent deuteron bombardment of the side walls of the target.

The neutron detector is mounted at a distance of 3 to 4 feet from the target on a remotely controllable angle changer, the pivot point of which is directly under the gas target. The selsyn control from the counting area permits accurate changes in steps of about 0.2° and is reproducible over long periods of time to better than 0.5°.

The neutrons are detected by means of a proton recoil counter telescope, similar in principle to others previously reported.[10,11] A schematic of its essential parts is shown in Fig. 2. Incident neutrons enter the detector and strike a thin polyethylene radiator. Knock-on protons in the forward direction pass through two gas-filled proportional counters (about one atmosphere argon-CO_2 mixture) and then deposit most of their energy in the $\frac{1}{8}$-in. thick, 1-in. diam CsI crystal. Several polyethylene radiators (all 1 inch in diameter) are available at different positions (six positions available) on the radiator wheel so that desired resolutions or counting rates may be obtained. One radiator wheel position contains a 1-in. diam carbon radiator and another position is open so that backgrounds due to the carbon in the polyethylene and to random events not associated with the polyethylene can be measured. The radiator wheel positions can be changed without affecting the cyclotron beam by means of a remotely controlled drive motor. Positive positioning of the radiator with respect to the proportional counters is obtained by having a corner of a properly aligned hexagonal positioning wheel close a microswitch when the radiator is in place, thus sending a signal to the counting area. The current passing through the helipot can also be read in the counting area, and the radiator in position is identified by this reading.

The energy distribution of the incident neutrons can be obtained by analyzing the pulse-height spectrum of those pulses in the CsI crystal which are in coincidence with pulses in the two proportional counters. One can thus separate the monoenergetic D(*d*,*n*)He³ neutron group from other neutrons present.

The neutron production is monitored by accumulating the charge collected by the gas target which is insulated from the beam pipe. Additional monitoring is done by another proton recoil counter telescope. This telescope contains only one proportional counter and one radiator,

[10] C. H. Johnson and C. C. Trail, Rev. Sci. Instr. **27**, 468 (1956).
[11] S. J. Bame, Jr., E. Haddad, J. E. Perry, Jr., and R. K. Smith. Rev. Sci. Instr. **28**, 997 (1957).

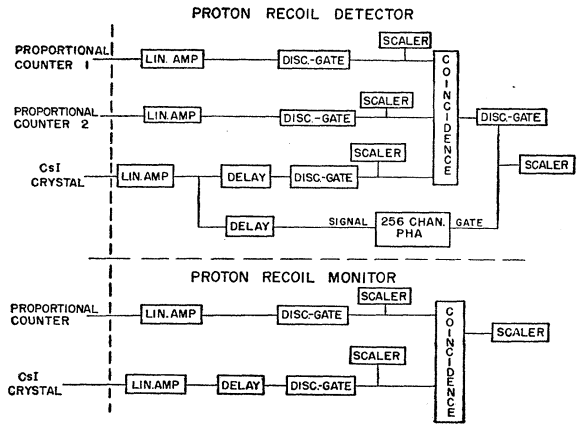

FIG. 3. Block diagram of the electronics associated with the proton recoil telescope detector and the proton recoil monitor.

and is maintained at a fixed position of about 15° to the incident deuteron beam (see Fig. 1). The bias setting on the discriminator in the crystal leg of the coincidence input can be varied until only neutrons from the monoenergetic *d*-D group are giving rise to coincidences. With this discriminator setting, a scaler on the output of the coincidence unit simply integrates the counts in the monoenergetic peak.

A block diagram of the electronics system is shown in Fig. 3. All components are standard microsecond circuitry.

In the early stages of the experiment, additional neutron production monitoring was done with a long counter and with a U^{238} fission chamber, but these were later dispensed with because of greater reliability of the current integrator and the proton recoil monitor.

The energy of the incident deuteron beam is determined by means of a differential range measurement. The range in aluminum is measured and then is converted to an energy by means of the range-energy relation of Aron *et al.*[12,13] Corrections are applied for the energy loss in the target foil and in one-half of the gas target. The uncertainty in the beam energy due to the range measurement, the intrinsic energy spread of the cyclotron beam, and drifting of the beam energy is about $\pm 2\%$.

ANGULAR YIELD MEASUREMENTS

A typical pulse-height spectrum from the proton recoil counter telescope, as viewed with a 256-channel pulse-height analyzer, is shown in Fig. 4. The incident energy is 12.2 Mev and the counter is at 0° with respect to the deuteron beam. The monoenergetic peak of neutrons from the D(d,n)He^3 reaction ($Q=+3.27$ Mev) can be clearly seen. At lower energy is the spectrum of neutrons resulting from the three-body "breakup" reaction D(d,pn)D (threshold$=-4.45$ Mev). Only the high-energy end of the breakup neutron spectrum is seen since the discriminator in the crystal leg into the triple coincidence unit is set to prevent lower energy breakup neutrons from giving rise to coincidences. The background due to neutrons not produced in the deuterium gas can be measured by running with the target evacuated, and this contribution can be readily subtracted.

It can be seen that setting the bias on the discriminator in the crystal leg of the proton recoil monitor at a point in the valley between the breakup and monoenergetic neutron groups will mean that the coincidence unit output, which is recorded on a scaler, will include all of the area under the monoenergetic peak, and we will be monitoring directly on the desired neutrons.

The angular resolution, as determined by the target size, proton radiator size, and the target-to-radiator spacing was about 1.5° at 0° and about 2.5° at 60° in the laboratory. The position of 0° was determined by taking data from about $-10°$, through 0° to positive angles and calling the peak position of the yield curve the true 0° position. The shape of the forward peak allowed an assignment of true 0° to about $\pm 1°$.

The measured angular yield curves are shown in Fig. 5, plotted in the center-of-mass system. The statistical uncertainty in the values ranges from about 2% at 0° to about 6% at angles in the minimum. The normalizations with respect to the integrated charge and the proton recoil monitor were both in agreement to within this accuracy, as were normalizations to the long counter and the fission chamber when they were used as auxiliary monitors. The Los Alamos data at 5.13

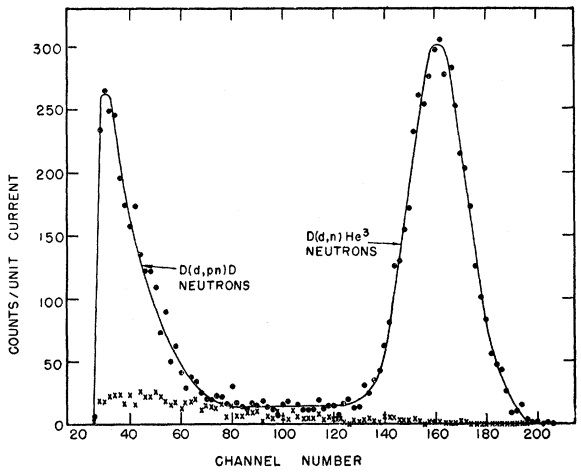

FIG. 4. A typical pulse-height spectrum from the proton recoil counter telescope. Deuteron energy$=12.2$ Mev. Neutron angle $=0°$. Circles denote deuterium gas in target; crosses designate evacuated target. The monoenergetic group of D(d,n)He^3 neutrons is well resolved from the high-energy end of the breakup neutron spectrum.

[12] W. A. Aron, B. G. Hoffman, and F. C. Williams, Atomic Energy Commission Report AECU-663 (2nd rev.), 1949 (unpublished). This report is also the University of California Radiation Laboratory Report UCRL-121 (2nd rev.), 1949 (unpublished).

[13] H. Bichsel, R. F. Mozley, and W. A. Aron, Phys. Rev. **105**, 1788 (1957).

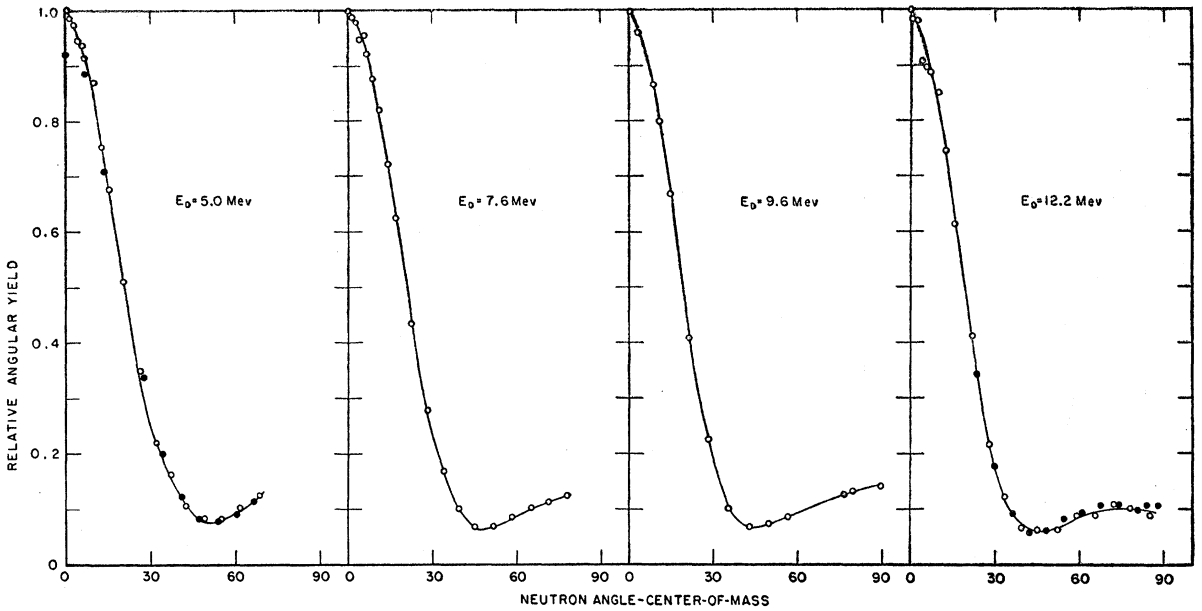

FIG. 5. Angular yield curves. The closed circles at 5.0 Mev are the 5.13-Mev data of Smith and Perry (reference 14) and at 12.2 Mev are the 12.2-Mev data of Brolley *et al.* (reference 2).

Mev, due to Smith and Perry,[14] have been plotted with the 5.0-Mev data, and were normalized to these data at a lab angle of 20.7°. The data of Brolley, Putnam, and Rosen[2] at 12.2±0.15 Mev have been plotted with the 12.2-Mev data, normalized at a lab angle of 30.1°. The agreement is seen to be excellent. The point at 79.4° on the 9.6-Mev curve was measured at 100.6° and then reflected through 90° to check the symmetry about 90°.

When the relative angular yield curves of Fig. 5 are made absolute by normalizing to the 0° cross-section measurements described in the next section, they can be fitted absolutely by a sum of even-order Legendre polynomials, $\sigma(\theta)=\sum_n a_n P_n(\cos\theta)$. The variation of the Legendre coefficients, a_n, with incident deuteron energy (Fig. 6) provides a means of constructing angular distribution curves for any energy through the range covered. The coefficients are listed in Table I, along with the integrated total cross sections. Polynomials to order $n=10$ were used, providing six parameters with which to fit the observed data. Excellent fits could be achieved, as seen in Fig. 7.

TABLE I. Legendre coefficients (in millibarns/steradian) resulting from fitting angular distributions with a sum of even-order Legendre polynomials. Total cross sections (in millibarns) from integration of the Legendre sum.

E_d (Mev)	a_0	a_2	a_4	a_6	a_8	a_{10}	σ_T
5.0	7.53	10.08	14.28	6.64	1.50	1.07	94.6
7.6	7.68	11.22	16.33	8.38	2.21	0.50	96.5
9.6	7.46	9.54	16.13	9.49	3.83	0.68	93.7
12.2	6.47	10.52	14.78	10.43	2.80	0.24	81.3

[14] R. K. Smith and J. E. Perry, Jr. (private communication).

Due to the identity of the incident and target particle in this reaction, the angular distribution is symmetric about 90° in the center-of-mass system. Therefore, conversion of the c.m. curves in Fig. 7 to the lab system provides angular distributions for all lab angles at these energies. Such curves are shown in Fig. 8. Since the 5.0-Mev curve is only measured to 70° in the c.m. system, the 5.0-Mev curve may be incorrect in the region from 50° to 90° in the lab system (dashed section in Fig. 8).

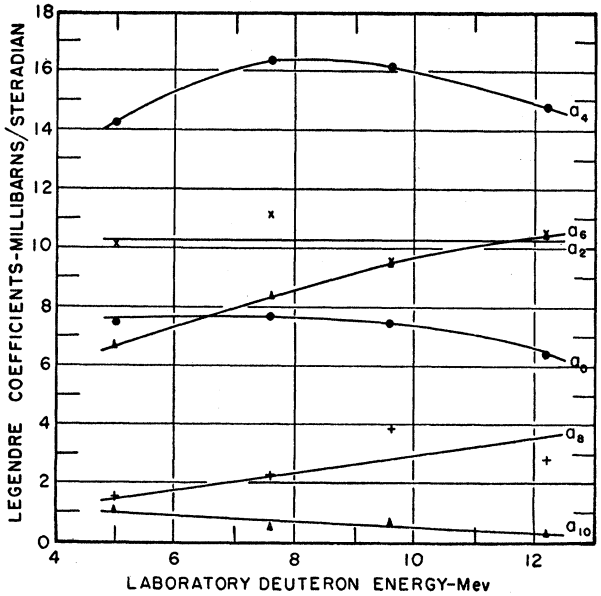

FIG. 6. Variation of the calculated Legendre coefficients with energy.

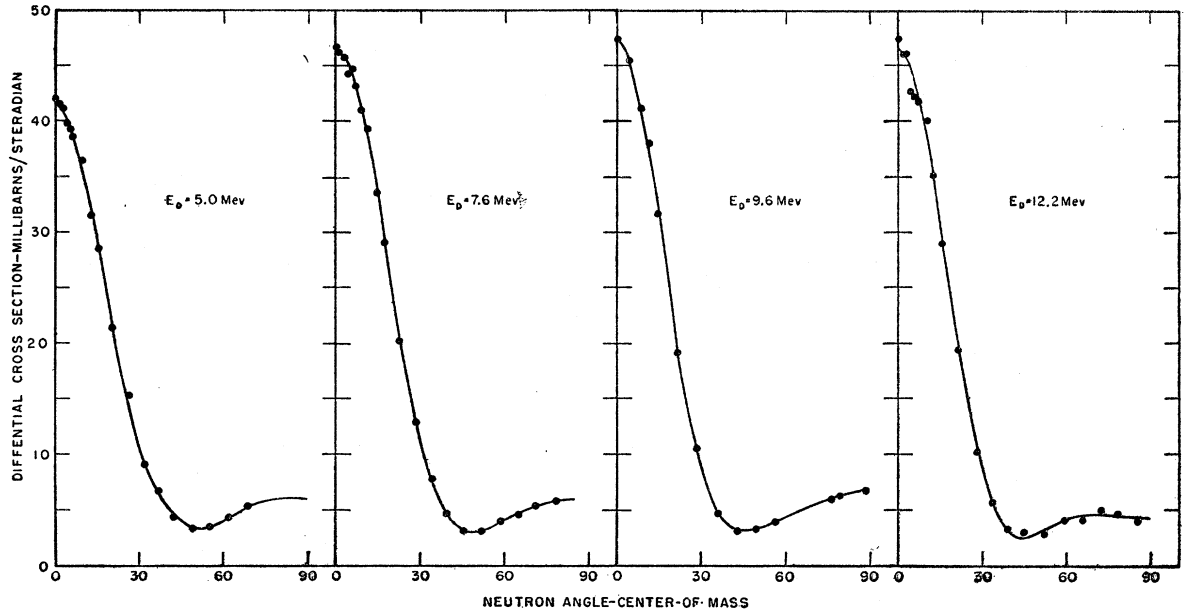

FIG. 7. The experimental data, transformed to the center-of-mass system and least-squares fit by a sum of Legendre polynomials.

ABSOLUTE CROSS SECTIONS

To measure the absolute cross sections at 0° the counter telescope was placed 40 inches from the center of the gas target and at 0° with respect to the deuteron beam. The polyethylene radiator was carefully weighed and measured and found to be 21.40 mg/cm² thick. The absolute efficiency of the telescope depends upon this radiator thickness, the internal geometry of the telescope, the differential *n-p* scattering cross section, and the solid angle subtended by the telescope radiator at the source. Bame *et al.*[11] express the absolute telescope efficiency, ϵ, as

$$\epsilon = P\sigma_T(E)M,$$

where P is the number of hydrogen atoms/cm² in the radiator, $\sigma_T(E)$ is the total *n-p* scattering cross section for neutrons of energy E, and M is a calculated quantity which contains the internal geometry, the target-radiator solid angle, and the anisotropy of *n-p* scattering.

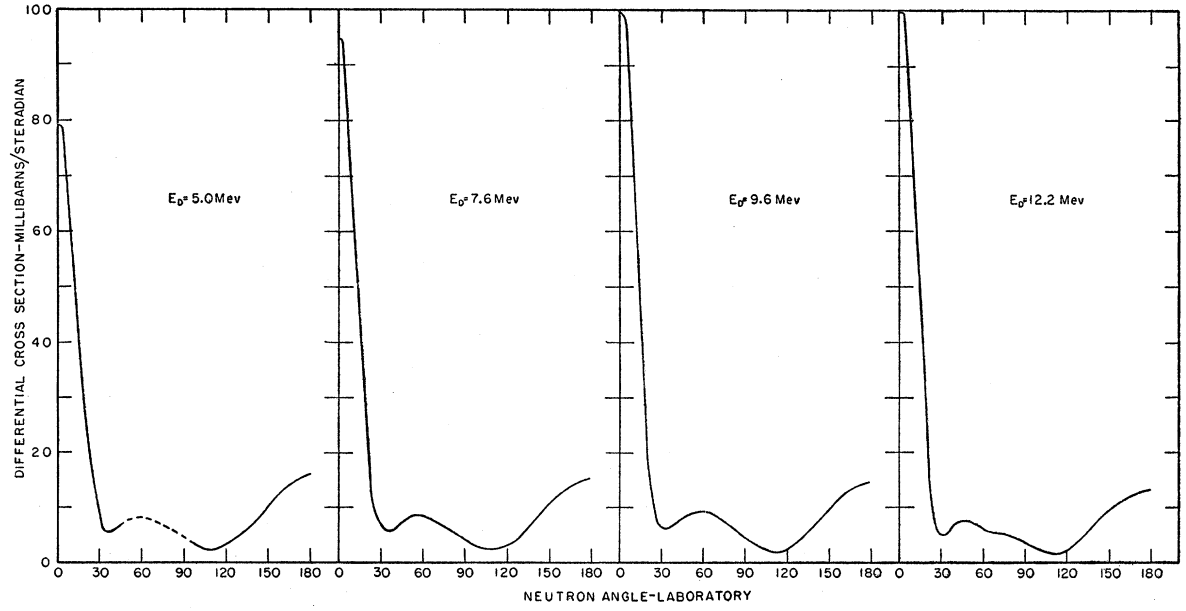

FIG. 8. The least-squares center-of-mass curves, transformed to the laboratory system. Use is made of the symmetry of the angular distribution about 90° in the center-of-mass system to define the cross section at all angles in the laboratory system. The dashed section in the 5.0-Mev curve is due to the lack of experimental data from 70° to 110° in the center-of-mass system.

Tables of M for a wide range of internal telescope parameters, target-radiator solid angles, and incident neutron energies, as well as interpolation methods, are given in reference 11. A semiempirical formula for calculating $\sigma_T(E)$, due to John Gammel, is also given in this reference. By means of this formula and the M tables, the absolute efficiency of the counter telescope used in this experiment was found to be of the order of 10^{-8}, and absolute efficiencies were obtainable with an estimated error of $\pm 3\%$, the largest uncertainty in this number being the n-p scattering anisotropy.

The deuterium gas was supplied by the Stuart Oxygen Company and was guaranteed to be 99.5% deuterium. An analysis determined the deuterium content to be $99.66\pm 0.05\%$. The target gas pressure was measured with a simple mercury column manometer. Frequent checks were made on the pressure, and

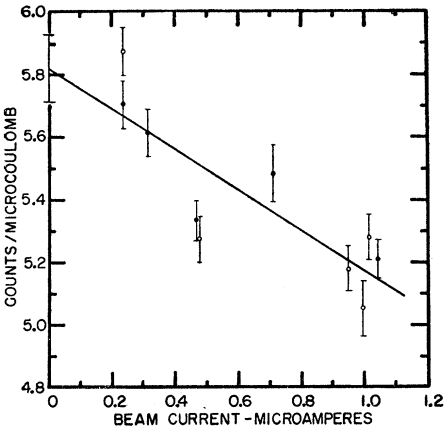

FIG. 9. Experimental determination of effect of beam heating on the density of deuterium atoms in the target. The zero beam level intercept can be determined to 2 or 3%. The open- and closed-circle points were obtained several days apart to check reproducibility.

the number of deuterium atoms/cm² in the target could be determined to an accuracy of $\pm 1\%$.

The deuteron beam was well collimated to a diameter of $\frac{1}{4}$ inch on entering the gas target. The loss of secondary electrons arising from deuteron passage through the 0.0005-in. tantalum entrance foil was suppressed by placing a 100-volt bias on an insulated section of beam pipe near the target entrance. Within statistics, no electron loss could be found with the bias removed.

The effect on the density of deuterium atoms in the target from heating due to passage of the deuteron beam through the gas was measured by running at several beam levels between 0.25 and 1.5 μa and extrapolating to zero beam level. A typical curve of the neutron counts in the telescope per μcoul of charge on the target versus beam level (Fig. 9) had a slope of approximately 0.5 counts/μcoul μa. The uncertainty in the zero beam level intercept was about 2 to 3%.

The measured absolute cross sections are listed in Table II. They have been corrected for the attenuation

TABLE II. Absolute cross sections for production of neutrons at 0°. The uncertainty in the incident deuteron energy is about $\pm 2\%$.

E_d (Mev)	$\sigma(0°)$ (mb/sr)
3.4	59.6±3.0
5.3	80.9±4.0
7.2	90.1±4.5
8.5	99.3±5.0
10.2	103.3±5.0

of the neutrons by the walls of the gas target and the entrance window of the counter telescope, a correction of about 2%. The correction due to the fact that the gas target is a line source rather than a point source, as assumed in the M table calculation, was found to be negligibly small (0.2%).

The absolute cross sections are plotted in Fig. 10. Also plotted are the preliminary data of Cochran, Smith, and Henkel,[15] from 6 to 14 Mev and the unpublished data of Smith and Perry,[14] from 0.5 to 6 Mev. Both sets of data were measured with a proton recoil telescope similar to the one used in this experiment, and the probable error in both sets is approximately 5%. The point at 8.4 Mev is that of Daehnick and Fowler.[3]

EXCHANGE STRIPPING THEORY

The exchange stripping approach of Owen and Madansky[8,9] was developed to account for the significant components in the backward direction found in some stripping angular distributions. In this approach the usual deuteron stripping theory[7,16] is modified to formally include contributions from "heavy-particle"

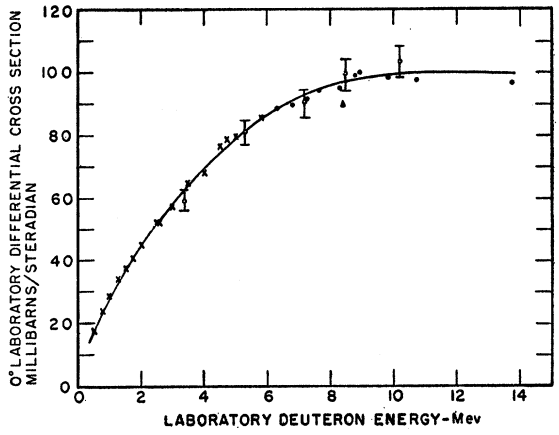

FIG. 10. Differential cross section at 0° in the laboratory system. The open circles are the present data, the closed circles are preliminary data of Cochran, Smith, and Henkel (reference 15), the crosses are unpublished data of Smith and Perry (reference 14), and the triangle is from Daehnick and Fowler (reference 3).

[15] D. R. F. Cochran, R. K. Smith, and R. L. Henkel (private communication). We very much appreciate permission to include these results prior to publication.

[16] A. B. Bhatia, K. Huang, R. Huby, and H. C. Newns, Phil. Mag. 43, 485 (1952).

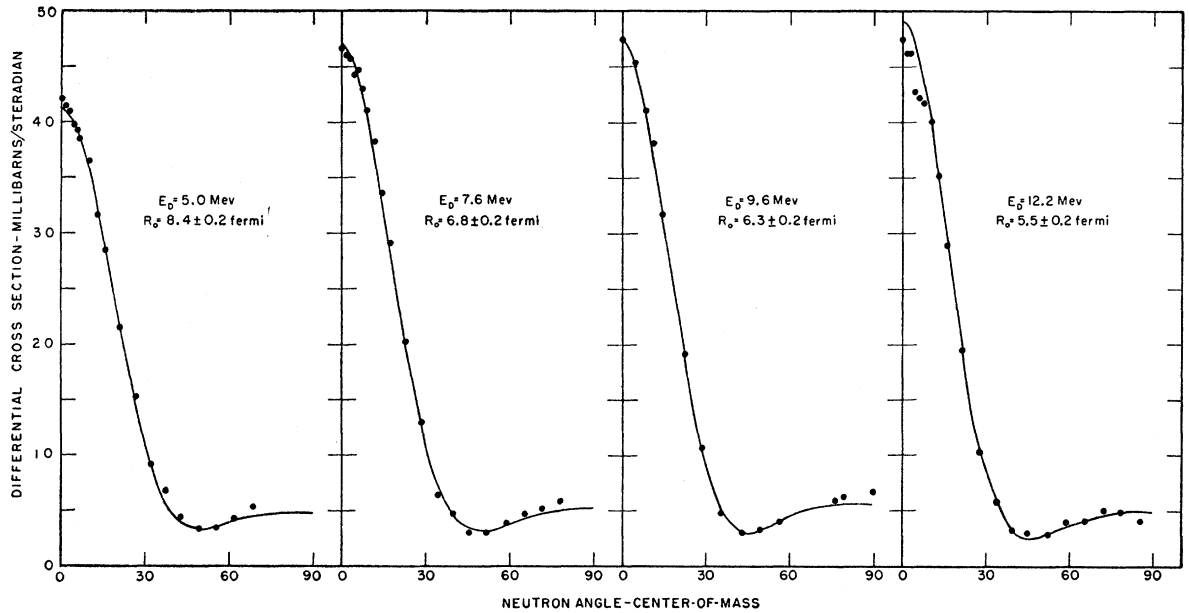

FIG. 11. The experimental data, with the best calculated exchange stripping fit at each energy. The stripping curves have been normalized to the data at 20°, and an isotropic component of about 3 millibarns/steradian has been added.

stripping. This is done by antisymmetrizing the final-state wave function for the outgoing neutron with respect to exchange of available neutrons in the deuteron and heavy particle. Since the $D(d,n)He^3$ reaction is unique in that both the incident and target particles must be equally regarded as the source of the resultant neutron, this approach should be particularly suitable to this reaction. The following relations result from the development of Daehnick and Fowler.[3]

A first-order Born approximation perturbation calculation yields a differential cross section which contains the incident deuteron stripping amplitude, the target deuteron (heavy particle) stripping amplitude, and an interference term between the two, i.e.,

$$\sigma(\theta) \propto h_d^2 + h_{d'}^2 - \tfrac{2}{3} h_d h_{d'}. \tag{1}$$

The interference term arises due to the fact that the neutron detector cannot distinguish between neutrons from the two deuterons. The $(-\frac{2}{3})$ coefficient of the interference term arises when the spin functions in the initial-state and final-state wave functions are properly combined.

The stripping amplitudes are spatial overlap integrals between initial- and final-state wave functions. They can be written as a product of three factors,

$$h_d \propto \Lambda G(K) f_l(k), \tag{2}$$

$$h_{d'} \propto \Lambda' G(K') f_l(k'). \tag{2'}$$

Λ is a measure of the reduced width for the formation of a final He^3 nucleus containing the target deuteron and the proton of the incident deuteron. Since it is not an angle dependent factor, it can be removed from the stripping amplitude for angular distribution fitting purposes.

$G(K)$ is the momentum transform of the neutron within the incident deuteron, with respect to the center of mass of the incident deuteron, and, in a zeroth-order square-well approximation, the angular dependent part has the form

$$G(K) \propto \left(\frac{8\pi\alpha_d}{\alpha_d^2 + K^2} \right)^{\frac{1}{2}}, \tag{3}$$

where

$$\alpha_d^2 \equiv M_n \epsilon_d / \hbar^2, \tag{4}$$

$$K^2 = |\vec{k}_n - \tfrac{1}{2}\vec{k}_d|^2. \tag{5}$$

α_d^2 is defined by the deuteron binding energy, ϵ_d. $\vec{k}_n$ and $\vec{k}_d$ are the wave vectors for the outgoing neutron and the incident deuteron, respectively.

$f_l(k)$ is the momentum transform of the internal spatial wave function of the final state of the captured proton relative to the target deuteron. Since the captured proton wave function is not strictly a plane wave, a delta-function interaction[16] at an interaction surface of radius R_0 is used to limit the integration. Distorting effects are not explicitly accounted for, but it is assumed that the interaction radius R_0 can be adjusted to simulate some of them. Since the proton is captured into an $l=0$ orbit in He^3, the angular-dependent part of $f_l(k)$ is given by a zero-order spherical Bessel function,

$$f_l(k) \propto j_0(kR_0), \tag{6}$$

$$k^2 = |\vec{k}_d - \tfrac{2}{3}\vec{k}_n|^2. \tag{7}$$

The wave vectors $\vec{K}$ and $\vec{k}$ contain the angle, θ, between the incident deuteron and the emitted neutron.

The factors $G(K')$ and $f_l(k')$ of Eq. (2') have forms identical to Eqs. (3) and (6), respectively. Since $\bar{k}_{d'}=-\bar{k}_d$, the wave vectors for the target deuteron stripping (the primed system) have the form

$$K'^2=|\bar{k}_n+\tfrac{1}{2}\bar{k}_d|^2, \quad (5')$$

$$k'^2=|-\bar{k}_d-\tfrac{2}{3}\bar{k}_n|^2. \quad (7')$$

EXCHANGE STRIPPING FITTING

When the proper forms for $G(K)$, $f_l(k)$, $G(K')$ and $f_l(k')$ [Eqs. (3) and (6), and their primed equivalents] are substituted into Eqs. (2) and (2'), it can be seen that the differential cross section expression, Eq. (1), contains only one adjustable parameter, the interaction radius R_0.

The measured data, with the best stripping fits at each energy, are plotted in Fig. 11. The fitting was done by normalizing the calculated curve to the least-square (Legendre) curve value at 20° and adding an isotropic component equal to the measured value at the minimum. The values of interaction radius, R_0, required to obtain the fit and the isotropic contribution at each energy are listed in Table III. The error of ±0.2 fermi

TABLE III. Values of the interaction radius, R_0, and the isotropic component required to obtain the best exchange stripping fit to the experimental data.

E_d (Mev)	R_0 (fermi)	Isotropic contribution (mb/sr)
5.0	8.4±0.2	3.3
7.6	6.8±0.2	3.0
9.6	6.3±0.2	3.1
12.2	5.5±0.2	2.3

(10^{-13} cm), indicated for the interaction radii, reflects the sensitivity of the fit of the forward peak to the choice of R_0.

A plot of the variation of the interaction radius with laboratory energy of the incident deuterons is shown in Fig. 12. The radius at 8.4 Mev is that of Daehnick and Fowler.[3] (The error on this point is approximate.) The radii at 3.0 and 14.0 Mev were obtained by constructing angular distributions at these energies by means of the Legendre coefficients of Brolley *et al.*[2] and treating these constructs the same as the experimentally measured curves.

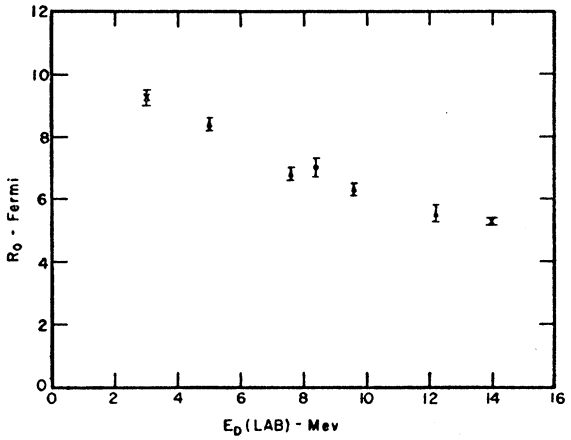

FIG. 12. The variation with energy of the interaction radii used to obtain the best exchange stripping fits. The triangles are from fits to the present data, the circles to the data of Daehnick and Fowler (reference 3) (error approximate) and the crosses to Legendre constructs from the data of Brolley *et al.* (reference 2).

As can be seen, there is a considerable change in R_0 over this energy range, and the values are quite high compared to the conventional deuteron "radius" of 4.3 fermi.[17] An analysis of the contributions made by the various distorting effects neglected in the development of the theory might lead to either a qualitative or quantitative explanation of the magnitude and variation of R_0.

Exchange stripping fits to the $N^{15}(d,n)O^{16}$ reaction[18] and the $B^{11}(d,n)C^{12}$ reaction[8,19] have also shown variations of R_0 with energy. It is well known that the stripping model is a relatively crude one, and it seems quite possible that radii obtained in this way can never be given any real physical significance.

ACKNOWLEDGMENTS

We wish to acknowledge the considerable assistance rendered by Erwin Schwarcz in the exchange stripping calculations. Thanks are also due to Donald Rawles for assisting in the data taking and reduction, to Bradley Johnston for coding the stripping fit problem for the IBM 650 calculator, and to the cyclotron crew under Leroy Erickson and Owen Tveitmoe. We are indebted to Jack M. Peterson for his continued interest and encouragement.

[17] J. M. Blatt and V. F. Weisskopf, *Theoretical Nuclear Physics* (John Wiley & Sons, Inc., New York, 1952), p. 52.
[18] J. L. Weil and K. W. Jones, Phys. Rev. 112, 1975 (1958).
[19] B. Zeidman and J. M. Fowler, Phys. Rev. 112, 2020 (1958).